

The theoretical justification is given of features of thermoacoustic effects, which is observed in a closed cylindrical tube during gas oscillations at resonance and near-resonance frequencies.

It is well known that oscillations of a gas column are capable of generating nonuniform heating of the tube walls. For large-amplitude oscillations the closed ends can heat up to 1000°K [1]. This effect is also observed for resonance oscillations in a tube open at one end [2, 3].

In the study of the thermoacoustic effect in a closed tube, undertaken in [1], it is assumed that in the frequency region far from resonance the theoretical description may be confined to the second approximation in series expansions in the small parameter $\varepsilon = U_\infty/\omega L \ll 1$. However, an error in the boundary conditions at the tube wall for the first approximation radial velocity component led to the loss of a most important term, so that the theoretical results of [1] do not describe the observed effect even qualitatively. At the same time, we are restricted in the resonance frequency region to the second approximation only, while the oscillation amplitude, on the other hand, can reach substantial values.

An attempt is made below to describe quantitatively the experimentally observed features of thermoacoustic effects in the whole frequency region investigated.

The equations describing the motion of a viscous, compressible fluid with constant physical properties in a long, cylindrical tube ($R/L \ll 1$) were given in [4]. To take into account absorption, which the wave undergoes during propagation, we introduce a complex wave number [5]

$$k = k_0(1 + i\eta),$$

so that the first approximation solution of the equations has the following form:

$$\begin{aligned} p_1 &= |C| \cos [k_0 x (1 + i\eta) + \alpha_r + \alpha_{im}] \exp(i\omega t), \\ u_1 &= -\frac{i|C|}{\rho_0 c_0} (1 + i\eta) \sin [k_0 x (1 + i\eta) + \alpha_r + \alpha_{im}] \times \\ &\quad \times \left[1 - \sqrt{\frac{R}{r}} \exp\left(- (1 + i) \sqrt{\frac{\omega}{2\nu}} (R - r)\right) \right] \exp(i\omega t), \\ v_1 &= \frac{\omega}{2\rho_0 c_0^2} \left\{ (2\eta + i\eta^2)(R^2 - r^2) \frac{1}{r} + (1 + i) \sqrt{\frac{2\nu}{\omega}} \left[\left((1 + i\eta)^2 + \frac{\kappa - 1}{\sqrt{\text{Pr}}} \right) \frac{R}{r} - (1 + i\eta)^2 \sqrt{\frac{R}{r}} \times \right. \right. \\ &\quad \left. \left. \times \exp\left(- (1 + i) \sqrt{\frac{\omega}{2\nu}} (R - r)\right) - \frac{\kappa - 1}{\sqrt{\text{Pr}}} \sqrt{\frac{R}{r}} \exp\left(- (1 + i) \sqrt{\frac{\omega \text{Pr}}{2\nu}} (R - r)\right) \right] \right\} p_1, \\ p_1 &= \frac{1}{c_0^2} \left[1 + (\kappa - 1) \sqrt{\frac{R}{r}} \exp\left(- (1 + i) \sqrt{\frac{\omega \text{Pr}}{2\nu}} (R - r)\right) \right] p_1, \\ T_1 &= \frac{1}{\rho_0 c_p} \left[1 - \sqrt{\frac{R}{r}} \exp\left(- (1 + i) \sqrt{\frac{\omega \text{Pr}}{2\nu}} (R - r)\right) \right] p_1, \end{aligned}$$

where the subscript denotes the corresponding approximation.

Let the closed end of the tube be located at the point $x = 0$, and let the piston oscillate around $x = L$, so that the boundary conditions are written in the form

V. I. Ul'yanov-Lenin Kazan State University. Translated from *Inzhenerno-Fizicheskii Zhurnal*, Vol. 47, No. 1, pp. 34-41, July, 1984. Original article submitted March 16, 1983.

$$u_1(x=0, r=0) = 0; u_1(x=L, r=0) = \omega l(\cos \varphi + i \sin \varphi) \exp(i\omega t).$$

Solving the system obtained, we find

$$\alpha_r = 0, \alpha_{im} = 0, |\bar{C}| = \frac{k_0 L l / L}{V(\eta^2 + 1)(\sin^2 k_0 L \operatorname{ch}^2 \eta k_0 L + \cos^2 k_0 L \operatorname{sh}^2 \eta k_0 L)}, \quad (1)$$

where $|\bar{C}| = |C|/\rho_0 c_0^2$, and consequently:

$$p_1 = \rho_0 c_0^2 |\bar{C}| \cos k_0 x (1 + i\eta) \exp(i\omega t),$$

$$u_1 = -i c_0 |\bar{C}| (1 + i\eta) \sin k_0 x (1 + i\eta) \left[1 - \sqrt{\frac{R}{r}} \exp\left(- (1 + i) \sqrt{\frac{\omega}{2\nu}} (R - r)\right) \right] \exp(i\omega t).$$

To determine η we use the energy balance equation. We assume that the amount of time-averaged energy introduced by the piston into the tube, W_1 , equals the amount of heat transferred through the tube walls into the surrounding medium due to thermoacoustic effects W_2 :

$$W_1 + W_2 = 0. \quad (2)$$

The work of the piston is calculated by the equation

$$W_1 = \pi R^2 \langle p_1(x=L) u_1(x=L, r=0) \rangle,$$

where $\langle \rangle$ denotes the time average. Calculating this expression, we obtain

$$W_1 = \frac{1}{4} \rho_0 c_0^3 \pi R^2 [\operatorname{sh} 2\eta k_0 L + \eta \sin 2k_0 L]. \quad (3)$$

The heat flow to the tube walls due to thermoacoustic effects can be calculated by the equation [3]

$$\langle q \rangle = - \left\langle \lambda \frac{\partial T_2}{\partial r} \right\rangle_R = - \frac{c_p \rho_0}{R} \left[\int_0^R r \frac{\partial \langle u_1 T_1 \rangle}{\partial x} dr + \int_0^R \frac{\partial \langle r v_1 T_1 \rangle}{\partial r} dr \right]. \quad (4)$$

Substituting the expressions for u_1 , T_1 , v_1 , we obtain after some transformations

$$\langle q \rangle = \frac{1}{8} \rho_0 c_0^2 |\bar{C}|^2 V \sqrt{2\nu\omega} [A \cos 2k_0 x + B \operatorname{ch} 2\eta k_0 x], \quad (5)$$

where

$$A = \frac{\kappa + 1 + 2\eta}{\sqrt{\operatorname{Pr}}} - 1 + 2 \frac{1 - \sqrt{\operatorname{Pr}} - \eta(1 + \sqrt{\operatorname{Pr}})}{1 + \operatorname{Pr}} - \eta^2,$$

$$B = \frac{\kappa - 1 + 2\eta - 2\eta^2}{\sqrt{\operatorname{Pr}}} + 1 - 2\eta \frac{1 + \sqrt{\operatorname{Pr}} + \eta(1 - \sqrt{\operatorname{Pr}})}{1 + \operatorname{Pr}} + \eta^2.$$

The total amount converted into thermal energy is found by integrating expression (5) over both tube surfaces

$$W_2 = - \frac{1}{4} \pi R L \rho_0 c_0^2 |\bar{C}|^2 V \sqrt{2\nu\omega} \left(A \frac{\sin 2k_0 L}{2k_0 L} + B \frac{\operatorname{sh} 2\eta k_0 L}{2\eta k_0 L} \right). \quad (6)$$

Substituting (3) and (6) into (2), we find the following relation for determining η :

$$\left(2 \frac{R}{\delta} \eta - B \right) \operatorname{sh} 2\eta k_0 L = - \eta \left(2 \frac{R}{\delta} \eta - A \right) \sin 2k_0 L,$$

where $\delta = \sqrt{2\nu/\omega}$.

Assuming that η is a small quantity, we neglect terms of order η^2 and higher, we use the relation $\operatorname{sh} 2\eta k_0 L \simeq 2\eta k_0 L$, and choosing for air $\kappa = 1.4$ and $\operatorname{Pr} = 0.72$, we obtain an expression for calculating η :

$$\eta = \frac{H \left(1.47 + 2 \frac{\sin 2k_0 L}{2k_0 L} \right)}{V k_0 L \left(1 + \frac{\sin 2k_0 L}{2k_0 L} \right)}, \quad (7)$$

where $H = (1/2R)\sqrt{2\nu L}/c_0$.

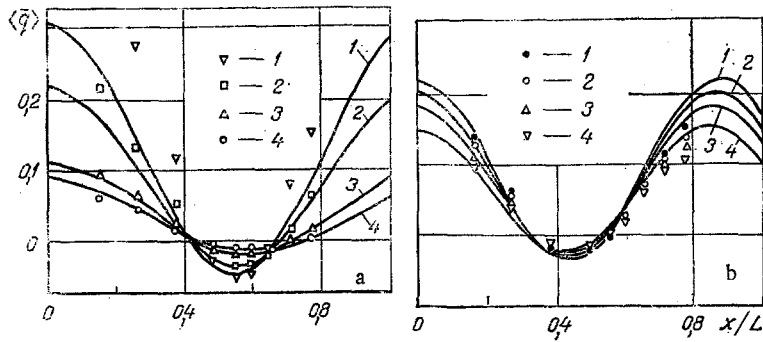


Fig. 1. Distribution of dimensionless thermal flow along the tube walls for frequencies below resonance (a) (1) $k_0L = 2.88$; 2) 2.83; 3) 2.71; 4) 2.59 and above resonance (b) (1) $k_0L = 3.59$; 2) 3.62; 3) 3.66; 4) 3.74). The curves are theory, and the points — the experimental data of [1].

Calculations show that the quantity η is indeed small (for the experimental set-up of [1] it is on the order of 10^{-2}). It cannot be totally discarded, however, since precisely this quantity restricts the amplitude value $|\bar{C}|$ at exact resonance:

$$|\bar{C}| = \frac{k_0 L l / L}{(\eta^2 + 1)^{\frac{1}{2}} \sin k_0 L}$$

Based on the results obtained, and restricting ourselves to second-order effects in describing thermoacoustic effects, we find the distribution of thermal flow along the tube walls, using (1), (5), and (7) for various k_0L , and compare with the experimental results of [1]. Figure 1a shows the theoretical and experimental results for frequencies below resonance, and Fig. 1b for frequencies above resonance, while Fig. 2 shows near-resonance results. As seen from these figures, the theory describes well the experimental results for k_0L below 2.83 and above 3.59: the wall heating at the closed ends, the cooling at the middle, and the shift of the cooling band as a function of frequency. In the range between these values the deviation between theory and experiment is enhanced, and at the resonance frequencies the theory, including second-order effects, does not agree with experiment even qualitatively (Fig. 2). This could be expected, since as resonance is approached the oscillation amplitude increases quickly, and the contribution of higher-order terms becomes substantial.

We attempt to take into account fourth-order effects, so as to describe thermoacoustic effects at resonance. In [3] this problem was considered for an open tube, where, due to the complexity of solving systems of equations of second and fourth orders, only terms resulting from the interaction of second-order quantities were retained in the fourth-order energy equation. The final expression for $\langle q \rangle$ with account of fourth-order terms was obtained in the following form [3] for $\kappa = 1.4$:

$$\begin{aligned} \langle q \rangle = & \frac{1}{8} \rho_0 c_0^2 |\bar{C}|^2 \sqrt{2\nu\omega} \left\{ 1.47 \operatorname{ch} 2\beta + \frac{|\bar{C}|^2}{4} [7.07 + 0.389 \operatorname{ch}^2 2\beta + \right. \\ & + 1.366 \operatorname{sh}^2 2\beta] + 2 \cos 2(k_0 x + \alpha_r) + \frac{|\bar{C}|^2}{4} [0.7 \sin 4(k_0 x + \alpha_r) - 4.54 \cos 4(k_0 x + \alpha_r) + 4.74 \sin^2 2(k_0 x + \alpha_r) \operatorname{sh} 2\beta - \\ & - 12.09 \cos 2(k_0 x + \alpha_r) \operatorname{ch} 2\beta - 1.4 \cos 2(k_0 x + \alpha_r) \operatorname{sh} 2\beta + \\ & \left. + k_0 x (3.36 \sin 2(k_0 x + \alpha_r) - 2.8 \cos 2(k_0 x + \alpha_r)) \operatorname{ch} 2\beta \right\}. \end{aligned} \quad (8)$$

In deriving the given expression, substantial simplification was achieved by introducing in the absorption calculation a linear x -dependence of the term $i\eta k_0 x$ with constant $i\beta$, which can be interpreted as a mean absorption coefficient. The same method is also used in solving the problem for a closed tube, and we compare the results with those obtained above for a complex wave number.

Introducing the mean absorption coefficient β leads to a simplified expression already in first order:

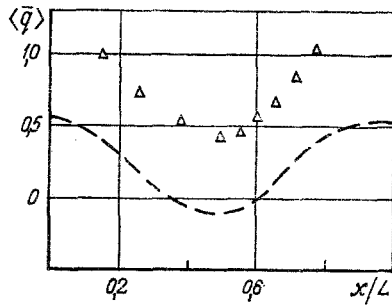


Fig. 2

Fig. 2. Dimensionless thermal flow along the tube walls near resonance. The points are experimental results for $k_0L = 3.36$ [1], and the dashed curve is second-order theory, not used in this case.

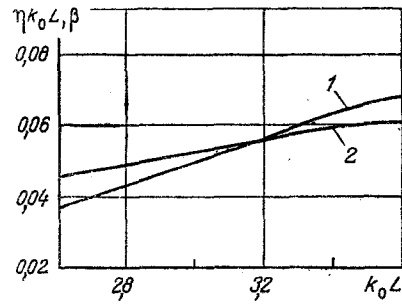


Fig. 3

Fig. 3. Dependence of ηk_0L (1) and β (2) on the dimensionless frequency k_0L .

$$p_1 = \rho_0 c_0^2 |\bar{C}| \cos(k_0 x + i\beta) \exp(i\omega t),$$

$$u_1 = -i c_0 |\bar{C}| \sin(k_0 x + i\beta) \left[1 - \sqrt{\frac{R}{r}} \exp\left(- (1+i) \sqrt{\frac{\omega}{2\nu}} (R-r)\right) \right] \exp(i\omega t),$$

$$v_1 = \frac{(1+i)\omega}{2\rho_0 c_0^2} \sqrt{\frac{2\nu}{\omega}} \left\{ \left(\frac{\kappa-1}{\sqrt{\text{Pr}}} + 1 \right) \frac{R}{r} - \sqrt{\frac{R}{r}} \left[\exp\left(- (1+i) \sqrt{\frac{\omega}{2\nu}} (R-r)\right) + \frac{\kappa-1}{\sqrt{\text{Pr}}} \exp\left(- (1+i) \sqrt{\frac{\omega \text{Pr}}{2\nu}} (R-r)\right) \right] \right\} p_1.$$

Repeating the behavior of the solution of the problem, we find an expression for the oscillation amplitude $|\bar{C}|$:

$$|\bar{C}| = \frac{k_0 L l / L}{\sqrt{\sin^2 k_0 L \text{ch}^2 \beta + \cos^2 k_0 L \text{sh}^2 \beta}}, \quad (9)$$

where β is determined by the relation

$$\left(2 \frac{R}{\delta} \beta - B k_0 L \right) \text{sh} 2\beta = \beta A \sin 2k_0 L,$$

and

$$A = \frac{2(1-\sqrt{\text{Pr}})}{1+\text{Pr}} + \frac{\kappa+1}{\sqrt{\text{Pr}}} - 1, \quad B = 1 + \frac{\kappa-1}{\sqrt{\text{Pr}}}.$$

For small values and in considering air β can be calculated by the equation

$$\beta = H \sqrt{k_0 L} \left(1.47 + 2 \frac{\sin 2k_0 L}{2k_0 L} \right). \quad (10)$$

Figure 3 shows graphically the dependences of the quantities ηk_0L and β on k_0L , calculated by Eqs. (7), (10) for the experiments of [1]. As is seen, their values at resonance coincide, but β increases more quickly with k_0L than ηk_0L . For $k_0L = 2.9$ and 3.4 the deviation in the ηk_0L and β values is less than 7%, but in this case the oscillation amplitude $|\bar{C}|$ is well described by the expression $|\bar{C}| = \frac{k_0 L l / L}{\sin k_0 L}$, coinciding with the equations of linear acoustics. The deviation in the numerical $|\bar{C}|$ values, calculated by Eqs. (1), (7), (9), and (10) for the experiments of [1], does not exceed 2%.

Thus, replacement of the complex wave number by the mean absorption coefficient leads to a change in the resonance $|\bar{C}|$ value by a quantity whose order is less than η . The deviation in the $|\bar{C}|$ values decreases with moving away from resonance. Therefore, the use of the mean absorption coefficient in considering thermoacoustic effects is fully justified, and, consequently, expression (8) retains its validity for a closed tube too, while in this case $\alpha_r = 0$, β is determined by Eq. (10).

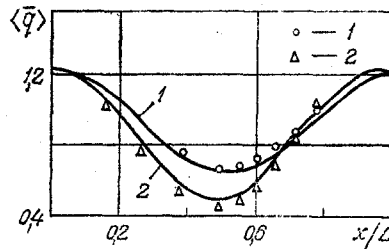


Fig. 4. Distribution of $\langle \bar{q} \rangle$ along the tube walls for resonance frequencies [1] $k_0L = 3.05$, 2) 3.24]. The curves are theory with account of fourth-order effects, and the points are the experimental data of [1] with account of the frequency shift.

Analysis of (8) shows that the main contribution of fourth-order effects to the treatment of thermal flow is provided by the second and ninth terms in the curly brackets. We recall that in obtaining expression (8) we did not take into account terms which are products of first and third orders, even though they also contain nonvanishing, time-averaged parts. Consequently, generalizing the contributions of fourth-order effects by the expression $|\bar{C}|^4$. ($a + b \cos 2k_0x$), the coefficients a and b need to be refined. For example, handling the experimental data obtained in [1] gives $a = -0.4$, $b = -25$. The expression to the tube walls during near-resonance oscillations ($2.83 < k_0L < 3.59$) for $Pr = 0.72$; $\kappa = 1.4$ acquires then the form

$$\langle q \rangle = \frac{1}{8} \rho_0 c_0^2 |\bar{C}|^2 \sqrt{2\nu\omega} [1.47 + 2 \cos 2k_0x - |\bar{C}|^2 (0.4 + 25 \cos 2k_0x)]. \quad (11)$$

Besides, it is necessary to take into account that thermoacoustic effects lead to gas heating, which is particularly strong near resonance frequencies. The temperature enhancement is due to the enhanced sound velocity, and, consequently, the resulting frequency shift. In considering near-resonance oscillations this frequency shift must be taken into account.

Figure 4 shows the distribution of thermal flow $\langle \bar{q} \rangle$ along the tube walls for near-resonance oscillations, calculated by Eq. (11) with account of the frequency shift, and the experimental data of [1]. As we see, good agreement is obtained between the results.

Thus, the augmented theory, taking into account fourth-order effects, allows quantitative description of the experimental features of thermoacoustic effects in the whole region of resonance and near-resonance frequencies.

NOTATION

R , tube radius; L , tube length; ϵ , a small parameter; U_∞ , maximum amplitude of velocity fluctuations; ω , frequency cycle; k , complex wave number; k_0 , real part of the wave number; η , coefficient taking into account absorption; p , pressure, u and v , axial and radial velocity components; t , time; x and r , axial and radial coordinates; ρ , density; α_r and α_{im} , constants determining the boundary conditions; $|\bar{C}|$, oscillation amplitude; c_0 , sound velocity in the unperturbed medium; ρ_0 , density of the unperturbed medium; Pr , Prandtl number; $\kappa = c_p/c_v$, specific heat ratio; ν , kinematic viscosity; T , gas temperature; z , piston displacement amplitude; φ , phase angle; W_1 , work of the piston; W_2 , thermal loss; $\langle q \rangle$, time-averaged thermal flux; λ , thermal conductivity coefficient; A , B , H , a , and b , constants; δ , width of the acoustic boundary layer; β , mean absorption coefficient; $\langle \bar{q} \rangle = \langle q \rangle (\mu c_0^2/R)^{-1}$, dimensionless thermal flux; and μ , dynamic viscosity coefficient.

LITERATURE CITED

1. P. Mercli and H. Thoman, "Thermoacoustic effects in a resonance tube," *J. Fluid Mech.*, **70**, 161-178 (1975).
2. R. G. Galiullin, I. P. Revva, and G. G. Khalimov, *Theory of Thermal Self-Oscillations* [in Russian], Kazan (1982).

3. R. G. Galiullin, I. P. Revva, and G. G. Khalimov, "Thermoacoustic effect in a resonant, semiopen tube," *Inzh.-Fiz. Zh.*, 43, 615-623 (1982).
4. R. G. Galiullin, I. P. Revva, and G. G. Khalimov, "Nonlinear gas oscillations in a semiopen tube," *Akust. Zh.*, 28, 617-621 (1982).
5. M. A. Isakovich, *General Acoustics* [in Russian], Nauka, Moscow (1973).

ELECTRONIC COMPUTER STUDY OF SEPARATION FLOW FEATURES
AROUND A VIBRATING CYLINDER

S. M. Belotserkovskii, V. N. Kotovskii,
M. I. Nisht, and R. M. Fedorov

UDC 533.695.5

The nonstationary separation flow around a circular cylinder performing harmonic vibrations across the stream by an incompressible viscous fluid is investigated in a numerical experiment.

Three qualitatively distinct regimes of separated flow around a circular cylinder performing harmonic vibrations perpendicularly to the free stream have been established by experimental means [1]. Regime I is neutral, for small dimensionless vibrations frequencies ($0 \leq Sh_1 \leq 0.04$), when their influence is not felt in the period of free vortex shedding from the cylinder, Regime II is transition ($0.04 \leq Sh_1 \leq 0.1$), and Regime III is "capture" ($Sh_1 > 0.1$) at which the frequency of free vortex shedding agrees with the frequency of cylinder vibration.

Among the theoretical papers in this area is [2] in which results of numerical experiments to compute the nonstationary separated flow of an ideal fluid around a vibrating cylinder are presented. However, this investigation is performed under the essential assumption about the site of stream separation on the cylinder surface since the separation points were not determined by a computation of the viscous flow in the boundary layer but were given in conformity with the experimental data for a selected Re number.

A method of modeling the nonstationary separation flow around bodies is proposed in [3, 4] on the basis of the synthesis of a scheme of an ideal medium and a boundary layer. Without any additional hypotheses not encompassed by these schemes, it permitted construction of the separation flow pattern around a fixed cylinder for both laminary and turbulent separation [4].

The present paper is devoted to modeling all the above-mentioned separation flow regimes around a vibrating cylinder on the basis of the same theoretical scheme. In addition to a phenomenological confirmation of the theoretical scheme, the authors tried to use a numerical experiment to set up the physical features of the phenomenon. It should be emphasized that the approach being developed possesses great generality and can be used not only for any profiles [3] but also for the study of spatial flows [5].

As in [3, 4], the flow as a whole around a cylinder is divided into a potential domain and a viscous flow domain in the boundary layer. The potential flow is computed by the method of discrete vortices [5]. Cumulative discrete vortices that replace the attached and free vortex layers are here arranged on the cylinder surface. The boundary conditions of nonpenetration of the cylinder surface were satisfied at the control points between the vortices.

In the presence of boundary layer separation from the cylinder surface, it is considered displaced completely at certain points in the potential flow domain in the form of free vortex sheets with intensity equal to the total boundary layer vorticity at its point of separation. Moreover, it is assumed that the discrete vortices by which the free vortex sheets are modeled move during the first step in time after boundary layer separation, at the average velocity of the center of vorticity of the boundary layer located at a distance of the displacement thickness from the streamline surface. At subsequent times they move together with the fluid and their circulations are conserved unchanged.

Translated from *Inzhenerno-Fizicheskii Zhurnal*, Vol. 47, No. 1, pp. 41-47, July, 1984.
Original article submitted April 29, 1983.